East European Journal of Physics. 1. 260-264 (2025)
DOI:10.26565/2312-4334-2025-1-29 ISSN 2312-4334

INFLUENCE OF IMPLANTATION OF ACTIVE METAL IONS ON THE COMPOSITION, EMISSION AND OPTICAL PROPERTIES OF MgO FILMS

M.B. Yusupjonova*, D.A. Tashmukhamedova, B.E. Umirzakov, S.S. Pak, Z.R. Saidakhmedova, Sh.K. Salieva
Tashkent State Technical University named after Islam Karimov, Tashkent, 100095 Republic of Uzbekistan
**Corresponding Author e-mail: ftmet@mail.ru*
Received November 26, 2024; revised January 21, 2025; accepted February 3, 2025

The composition, electronic structure, emission and optical properties of MgO/Mg films implanted with Ba+ and Na+ ions before and after annealing were studied by using a combination of secondary and photoelectron spectroscopy methods. It has been shown that after ion implantation, amorphous films consisting of Mg – Ba – O, Mg – O, Ba – O compounds, as well as unbound Ba and Mg atoms, are formed in the surface layers. In this case, eφ of the surface decreases. It has been determined that the emission efficiency of ion-doped layers is higher than that of MgO layers. Post-implantation annealing at T = 900 K leads to the formation of a homogeneous $Mg_{0.4}Ba_{0.6}O$ film with a thickness of 30 – 35 Å in the case of Ba^+ ion implantation. It has been revealed that the photoelectron escape depth λ of the three-component film is 1.5 times greater than that of Mg oxide. The main mechanisms of changes in the electronic structure, emission and optical properties of MgO during ion implantation and subsequent annealing have been identified.
Keywords: *Thermal oxidation; Ion implantation; Photoelectron spectroscopy; Quantum yield; Emission efficiency; Yield depth*
PACS: 61.72.uj, 68.55.Ln

INTRODUCTION

Metal oxides are promising in various fields of electronics and electronic engineering [1–5], in particular, photoelectric devices, ultraviolet photodetectors, sensors, thermal and electrical insulators, semiconductors, fuel cell additives, antimicrobial materials, optical electronics and nanoelectronics. The unique physical properties of high-quality magnesium oxide films allow them to be used as buffer layers and substrates for superconducting coatings [6], for structures based on wide-bandgap semiconductors [7], in spintronics devices [8], protective layer of plasma display panels [9], one of the materials for pyrochemical technology of spent nuclear fuel reprocessing [10, 11] and as coatings for spacecraft [12].

Various methods have been used to create and study thin MgO films: high-frequency sputtering [13 – 15], thermal treatment [16, 17], chemical spray pyrolysis [18 – 20], laser ablation [21], arc plasma melting [22], and aerosol assisted chemical vapor deposition technique [23].

The spatial distribution of structural features of MgO film on sapphire was determined in combination with X-ray structural analysis and layer-by-layer plasma etching and the presence of a thin transition layer with signs of rhombohedral deformation has been revealed in [13]. High transparent and antireflective properties of MgO thin film with an average transmittance of about 91.48% in the visible range, as well as a high reflectivity in the IR range have been found by the authors of [19]. These results can be used as an optical window or a buffer layer, and a well-reflective surface will prevent an increase in surface temperature under the influence of solar radiation, which can be used in solar cell applications.

We have previously studied the processes of formation of nanosized phases on the Si and GaAs surface during implantation of Ba^+, Na^+ and O^+_2 ions [24 – 27]. We have also studied the effect of implantation of active metal ions on the composition, structure, emission and electrophysical properties of SiO_2 and CaF_2 films [28 – 30].

However, investigations on obtaining nanosized phases and films on the surface of MgO films using the ion implantation method have not been conducted yet. The composition, crystal and electronic structure, emission and optical properties of thin films of Mg oxides with nanosized structures have not practically been studied.

This article will present the results of experimental studies on the effect of low-energy (E_0 = 0.5 – 5 keV) implantation of Ba^+ and Na^+ ions on the composition, structure, and physical properties of MgO/Mg films.

EXPERIMENTAL TECHNIQUE

All technological impacts (Mg oxidation, temperature treatment, ion implantation) and studies of the composition, electronic structure and physical properties have been carried out in the same ultra-high vacuum device. MgO films have been obtained by thermal oxidation of Mg. MgO with a thickness of θ = 800 Å has mainly been used. Before oxidation, Mg has been outgassed at T = 1,200 K under a vacuum of 10^{-7} Pa for 5–6 hours. Then, O_2 molecules have been admitted to the device to a pressure of $5 \cdot 10^{-3}$ Pa, which fell on the Mg surface heated at T = 1,000 K. Active metal ions Ba^+ and Na^+ have been created by surface ionization.

Cite as: M.B. Yusupjonova, D.A. Tashmukhamedova, B.E.Umirzakov, S.S. Pak, Z.R. Saidakhmedova, Sh.K. Salieva, East Eur. J. Phys. 1, 260 (2025), https://doi.org/10.26565/2312-4334-2025-1-29

The elemental and chemical composition of the nanofilms has been determined by Auger electron spectroscopy (AES), and the electronic structure has been determined by ultraviolet photoelectron spectroscopy (UPES). The error in determining the atomic concentration was ~ 5 – 8 at.%. To determine the depth distribution profile of impurities, layer-by-layer Auger analysis has been performed by sputtering the sample surface with 1 keV Ar^+ ions at an incidence angle of ~ 80° relative to the normal; the etching rate was ~ (3 ± 1) Å/min. The quantum yield of photoelectrons Y has been measured at a photon energy of hν ≈ 10.8 eV. The energy dependence of the secondary electron emission coefficients (SEEC) σ has been measured in the primary electron energy range of E_p = 100 – 1500 eV.

EXPERIMENTAL RESULTS AND DISCUSSION

The MgO/Mg system was outgassed at T = 800 K for 2 – 3 hours before the research. Implantation of Ba^+ and Na^+ ions was performed with the energy E_0 = 1 keV at the saturation dose D = $6\cdot10^{16}$ cm^{-2} in a vacuum of $5\cdot10^{-7}$ Pa at room temperature. The composition, structure and physical properties of the ion-implanted sample do not change significantly starting from D = $6\cdot10^{16}$ cm^{-2}, i.e. this dose is the saturation dose $D_н$. Table 1 shows the emission parameters of MgO/Mg films with a thickness d = 800 Å, before and after ion implantation, where σ_m is the maximum value of σ, λ is the depth of the yield of true secondary and photoelectrons. It is evident that after ion implantation the values of σ_m, Y and λ increase noticeably. This can be explained by the fact that compounds of the Mg – O, Me – O, Mg – Me – O type are formed, as well as unbound Mg and Me (Ba or Na) atoms in the ion-implanted layer. In this case, excess Ba (Na) atoms with a thickness of 0.5 – 0.6 monolayers are formed on the surface, which leads to a decrease in the work function of the surface. Apparently, the emission efficiency of Ba + O and Ba + Mg + O compounds is significantly higher than the emission efficiency of MgO. All this leads to a noticeable increase in the depth of the yield of true secondary and photoelectrons, therefore, the values of σ_m and Y increase to 1.5 – 2 times (see Table 1).

Table 1. Emission parameters of MgO before and after implantation of $Ba^+$and Na^+ ions with E_0=1 keV, D=$6\cdot10^{16}$ cm^{-2}

Subject of research	σ_m	E_{pm}, eV	η at (E_p = 500 eV)	Y at hν = 10.8 eV	λ, Å
MgO	3.9	800	0.22	$3\cdot10^{-4}$	400
$Ba^+ \rightarrow$ MgO	7.2	1000	0.32	$6\cdot10^{-4}$	600
$Na^+ \rightarrow$ MgO	8.1	1000	0.25	$7\cdot10^{-4}$	600

Thus, the growth of σ_m of magnesium oxide after implantation of sodium and barium ions can be caused by a decrease in eφ, an increase in λ and the formation of an oxide film with a comparatively high emission efficiency.

Post-implantation annealing was carried out at different temperatures in order to obtain a homogeneous three-component film with good stoichiometry. The temperature of 900 K was optimal for obtaining a polycrystalline Mg + Ba + O film. Fig. 1 shows the initial part of the Auger spectra of pure Mg, an MgO/Mg film, an MgO film bombarded with Ba^+ ions with E_0 = 1 keV at D = $D_н$ and heated at T = 900 K for 40 min, and the Auger spectrum of a thick BaO film is shown for comparison.

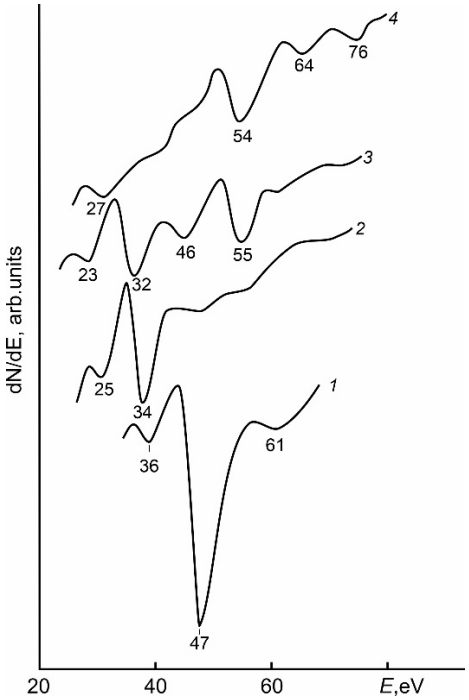

Figure 1. Auger spectra: 1 – pure Mg, 2 – Mg with MgO film, 3 – MgO implanted with Ba^+ ions with E_0 = 1 keV and heated at T = 900 K for 40 min, 4 – thick BaO/Mg film

It is evident that during the formation of the MgO film, the $L_{23}VV$ peak (47 eV) of Mg shifts sharply toward lower energies and other peaks characteristic for MgO appear. Analysis of the full spectrum of MgO showed that all peaks characteristic for Mg disappear in this case. After bombardment with Ba^+ ions and subsequent annealing, the main peak of MgO observed at E = 34 eV shifts toward lower energies by 2 eV. New peaks also appear at energies of 23, 46 and 55 eV. The positions and shapes of these peaks differ from those for a thick BaO film. It can be assumed that compounds of the Mg + Ba + O type are formed in this case. To estimate the concentration of atoms, we used high-energy Auger peaks of Mg (1189 eV), Ba (584 eV), O (503 eV) and determined the concentrations of these elements using the formula $C_x = \frac{I_x/S_x}{\sum I_i/S_i}$.

Figure 2 shows the distribution profiles of Ba, Mg and O atoms by depth h for MgO implanted with Ba^+ ions with E_0 = 1 keV at D = $6 \cdot 10^{16}$ cm^{-2} and heated at T = 900 K for 40 min. It is evident from Figure 2 that after heating at T = 900 K, the surface concentrations of Mg, Ba and O are ~ 18 – 20, 30 – 32 and 48 – 50 at.%, respectively. It is possible to assume that a three-component compound with the approximate composition $Mg_{0.4}Ba_{0.6}O$ is formed on the surface of MgO in this case. These concentrations do not change significantly to a depth of 35 – 40 Å, i.e. a $Mg_{0.4}Ba_{0.6}O$ film with a thickness d = 35 – 40 Å is formed. The Ba concentration decreases monotonically from ~ 20 – 25 at.% to zero, and the Mg concentration increases from 30 – 35 at.% to 50 – 52 at.% in the range of h = 40 – 80 Å. In the studied region of h, the O concentration does not change noticeably and is ~ 50 – 52 at.%.

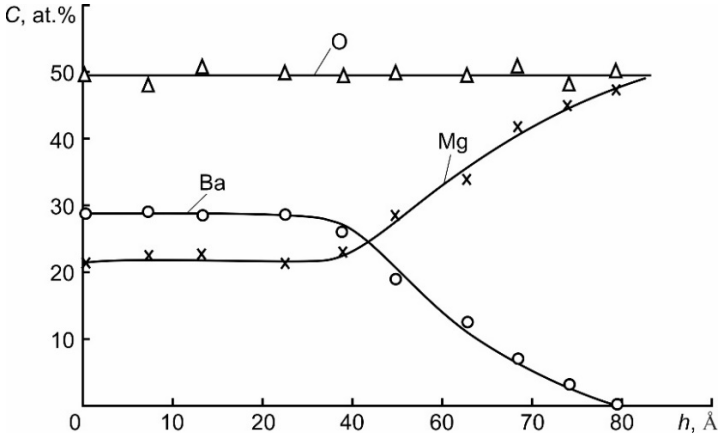

Figure 2. Profiles of the distribution of Mg, Ba and O atoms by depth h for MgO implanted with Ba^+ ions with E0 = 1 keV at D = $6 \cdot 10^{16}$ cm^{-2} and heated at T = 900 K.

Fig. 3 shows the photoelectron spectra for a MgO film and MgO with a $Mg_{0.4}Ba_{0.6}O$ nanofilm, recorded at hν = 15.6 eV. It is evident that the MgO spectrum has 2 maxima at E_b = – 1.5 eV and – 6.2 eV, respectively, caused by the excitation of electrons from the 3s states of Mg electrons and the 2p states of O electrons. The peculiarity in the region of E_b = – 3.8 eV can be associated with the hybridization of the 3s states of Mg with the 2p state of O. The spectrum width ΔE for MgO is ~ 7.4 eV. Using the formula hν = ΔE + Φ, we can determine Φ, which is ~ 8.2 eV. Here Φ is the photoelectron work function, the value of which is $E_{vac} – E_V$; E_B is the vacuum level, E_V is the top of the valence band.

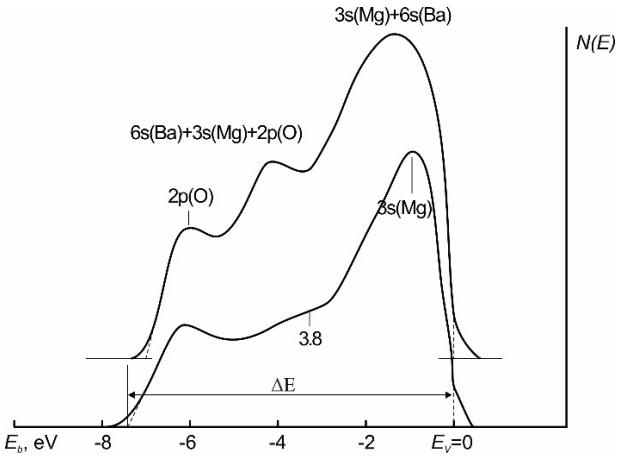

Figure 3. Photoelectron spectra: 1 – MgO/Mg; 2 – $Mg_{0.4}Ba_{0.6}O$/MgO/Mg

If we take into account that χ (electron affinity) for MgO is ~1.0 eV [31], then the band gap width $E_g = E_V$ - χ = 7.2 eV. The spectrum contains 3 maxima in the case of the $Mg_{0.4}Ba_{0.6}O$ film. Here, the spectrum width

decreases by ~ 0.4 eV, and the area under the curve (i.e., the quantum yield of photoelectrons) increases by ~ 1.4 – 1.5 times. Possible interpretations of the formation of maxima are shown in curve 2.

Table 2 shows the band-energy parameters of MgO and $Mg_{0.4}Ba_{0.6}O$ films. It is evident that the values of E_g, σ_m and Y of the three-component film are significantly greater than those of the MgO film.

Table 2. Band-energy parameters and values of σ_m and Y

Films	Structure	Thickness, Å	Φ, eV	E_g, eV	χ, eV	σ_m	Y
MgO/Mg	polycrys.	800	8.2	7.2	1.0	3.9	$3\cdot10^{-4}$
$Mg_{0.4}Ba_{0.6}O$/MgO	polycrys.	40	8.6	7.8	0.8	5.5	$5\cdot10^{-4}$

CONCLUSIONS

1. It has been shown that low-energy implantation of Ba^+ and Na^+ ions leads to a significant increase in the maximum value of the SEE coefficients and the quantum yield of photoelectrons. The main mechanisms leading to these changes have been revealed.
2. The method of implantation of Ba^+ ions into MgO with subsequent annealing has been used to obtain and determine the optimal conditions (energy and dose of ions, temperature of post-implantation annealing) for the synthesis of $Mg_{0.4}Ba_{0.6}O$ type films for the first time.
3. It has been pointed that the density of state of valence electrons and the parameters of the energy bands of MgO and $Mg_{0.4}Ba_{0.6}O$ differ significantly from each other.

ORCID

M.B. Yusupjonova, https://orcid.org/0000-0003-1189-687X; **D.A. Tashmukhamedova,** https://orcid.org/0000-0001-5813-7518
B.E. Umirzakov, https://orcid.org/0000-0002-9815-2111; **S.S. Pak,** https://orcid.org/0009-0004-0229-3895
Z.R. Saidakhmedova, https://orcid.org/ 0009-0003-5363-7590; **Sh.K. Salieva,** https://orcid.org/0009-0004-4022-9309

REFERENCES

[1] G. Balakrishnana, R. Velavana, K.M. Batoob, and E.H. Raslan, "Microstructure, optical and photocatalytic properties of MgO nanoparticles," Results Phys. **16**, 103013 (2020). https://doi.org/10.1016/j.rinp.2020.103013
[2] D. Lu, Q. Jiang, X. Ma, K. Wang, X. Fu, Y. Huang, and B. Hou, "Characterization of Zn in a polycrystalline MgO film Mater," Charact. **173**, 110955 (2021). https://doi.org/10.1016/j.matchar.2021.110955
[3] B. Nagappa, and G.T. Chandrappa, "Mesoporous nanocrystalline magnesium oxide for environmental remediation," Microporous Mesoporous Mater. **106**, 212-218 (2007).
[4] C.H. Park, J.Y. Choi, M.S. Choi, Y.K. Kim, and H.J. Lee, "Effects of MgO thin film thickness and deposition rate on the lifetime of ac plasma display panel," J. Surf. Coat. Technol. **197**, 223-228 (2005).
[5] F.M. Tezel, U. Veli, and I.A. Kariper, "Synthesis of MgO thin films: How heat treatment affects their structural, electro-optical, and surface properties," Materialstoday Communication, **33**, 104962 (2022). https://doi.org/10.1016/j.mtcomm.2022.104962
[6] I.M. Kotelyansky, V.B. Kravchenko, V.A. Luzanov, and A.T. Sobolev, Bull. Materials Sci. **14**(2), 479 (1991). (in Russian)
[7] Y. Chen, H. Ko, S. Hong, and T. Yao, "Layer-by-layer growth of ZnO epilayer on Al_2O_3(0001) by using a MgO buffer layer," Appl. Phys. Lett. **76**(5), 559-561 (2000). https://doi.org/10.1063/1.125817
[8] W.H. Butler, X.-G. Zhang, T.C. Schulthess, and J.M. MacLaren, "Spin-dependent tunneling conductance of Fe|MgO|Fe sandwiches," Phys. Rev. **63**(5), 054416 (2001). https://doi.org/10.1103/PhysRevB.63.054416
[9] A.I. Ektessabi, H. Nomura, N. Yasui, and Y. Tsukuda, "Ion beam processing of MgO thin films," Thin Solid Films, **447–448**, 383-387 (2004). https://doi.org/10.1016/S0040-6090(03)01092-7
[10] O.A. Golosov, S.S. Khvostov, N.V. Glushkova, M.V. Evseev, S.V. Staritsy, Yu.P. Zaikov, V.A. Kovrov, *et al*., "Corrosive and mechanical resistance of MgO ceramics under metallizing and mild chlorination of spent nuclear fuel in molten salts," Ceramics International, **47**(3), 3306-3311 (2021). https://doi.org/10.1016/j.ceramint.2020.09.171
[11] Zh. Xu, U. Eduok, and J. Szpunar, "Effect of annealing temperature on the corrosion resistance of MgO coatings on Mg alloy," Surf. Coating. Technol. **357**, 691-697 (2019). https://doi.org/10.1016/j.surfcoat.2018.10.076
[12] M.M. Mikhailov, and V.A. Goronchko, "Optical properties and radiation stability of polypropylene modified with MgO nanoparticles," Spacecrafts & Technologies, **6**(2), 102-108 (2022). https://doi.org/10.26732/j.st.2022.2.04
[13] V. A. Luzanov, "Growth Features of Thin Epitaxial Magnesium Oxide Films on Sapphire," Journal of Communications Technology and Electronics, **64**(7), 720–721 (2019). https://doi.org/10.1134/S1064226919070118
[14] B.Ç. Toprak, H.İ. Efkere, S.Ş. Aydın, *et al*., "Structural, morphological, optical and electrical characterization of MgO thin films grown by sputtering technique on different substrates," J. Mater. Sci: Mater Electron, **35**, 1389 (2024). https://doi.org/10.1007/s10854-024-13116-z
[15] D. Cáceres, I. Colera, I. Vergara, R. González, and E. Román, "Characterization of MgO thin films grown by rf-sputtering," Vacuum, **67**(3–4), 577-581 (2002). https://doi.org/10.1016/S0042-207X(02)00251-8
[16] T.T. Magkoev, G.S. Grigorkina, V.B. Zaalishvili, O.G. Burdzieva, E.N. Kozyrev, G.E. Tuaev, and K. Fukutani, "Feature of the MgO(111) Surface As a Substrate for Deposited Nanosized Au Particles in the Adsorption and Interaction of CO, NO, and O_2 Molecules," Russian Journal of Physical Chemistry A, 94(2), 401–404 (2020). https://doi.org/10.1134/S0036024420010203
[17] G.P. Panasyuk, E.A. Semenov, I.V. Kozerozhets, Kh.E. Yorov, L.A. Azarova, and A.I. Khol'kin, "A New Method of Synthesis of Nanosized Metal Oxide Powders," Doklady Chemistry, **482**, Part 1, 201–203 (2018). https://doi.org/10.1134/S0012500818090033
[18] M.H. Al-Timimi, W.H. Albanda, and M.Z. Abdullah, "Influence of Thickness on Some Physical Characterization for Nanostructured MgO Thin Films," East Eur. J. Phys. (2), 17 (2023). https://doi.org/10.26565/2312-4334-2023-2-17

[19] M. Tlili, C. Nefzi, B. Alhalaili, C. Bouzidi, L. Ajili, N. Jebbari, R. Vidu, *et al*., "Synthesis and Characterization of MgO Thin Films Obtained by Spray Technique for Optoelectronic Applications," Nanomaterials, **11**(11), 3076 (2021). https://doi.org/10.3390/nano11113076
[20] O.V. Diachenko, A.S. Opanasuyk, D.I. Kurbatov, N.M. Opanasuyk, O.K. Kononov, D. Nam, H. Cheong // ACTA PHYSICA POLONICA A. 2016. V. 130. No. 3. P. 805 – 810. https://doi.org/10.12693/APhysPolA.130.805
[21] P. Płóciennik, D. Guichaoua, A. Zawadzka, A. Korcala, J. Strzelecki, *et al*., "Optical properties of MgO thin films grown by laser ablation technique," Optical and Quantum Electronics, **48**(5), 277 (2016). https://dx.doi.org/10.1007/s11082-016-0536-8
[22] A. Kruk, "Fabrication of MgO high transparent ceramics by arc plasma synthesis," Opt. Mater. **84**, 360 (2018). https://doi.org/10.1016/j.optmat.2018.07.001
[23] S.D. Ponja, I.P. Parkin, and C.J. Carmalt, "Magnesium Oxide Thin Films with Tunable Crystallographic Preferred Orientation via Aerosol-Assisted CVD," Chemical Vapor Deposition, **21**(4-5-6), 145-149 (2015). https://doi.org/10.1002/cvde.201507156
[24] B.E. Umirzakov, D.A. Tashmukhamedova, and K.K. Kurbanov, "Estimation of changes in parameters of a crystal lattice and energy bands upon variation in the size of nanocrystals and nanofilms of silicides prepared by ion implantation," Journal of Surface Investigation, **5**(4), 693 (2011). https://doi.org/10.1134/S1027451011070214
[25] D.A. Tashmukhamedova, "Study of composition and electronic structure of $CoSi_2$/Si interface," Bulletin of the Russian Academy of Sciences: Physics, **70**(8), 1409 (2006).
[26] Z.A. Isakhanov, Z.E. Mukhtarov, B.E. Umirzakov, and M.K. Ruzibaeva, "Optimum ion implantation and annealing conditions for stimulating secondary negative ion emission," Technical physics, **56**(4), 546-549 (2011). https://doi.org/10.1134/S1063784211040177
[27] Kh.Kh. Boltaev, Zh.Sh. Sodikjanov, D.A. Tashmukhamedova, B.E. Umirzakov, "Composition and Structure of $Ga_{1-x}Na_xAs$ Nanolayers Produced near the GaAs Surface by Na^+ Implantation," Technical Physics, **62**(12), 1882-1884 (2017). https://doi.org/10.1134/S1063784217120040
[28] M.B. Yusupjanova, D.A. Tashmukhamedova, and B.E. Umirzakov, "Composition, morphology, and electronic structure of the nanophases created on the SiO_2 Surface by Ar^+ ion bombardment," Tech. Phys. 61, 628-630 (2016). https://doi.org/10.1134/S1063784216040253
[29] B.E. Umirzakov, T.S. Pugacheva, A.K. Tashatov, and D.A. Tashmuchamedova, "Electronic structure and optical properties of CaF_2 films under low energy Ba^+ ion-implantation combined with annealing," Nuclear Instruments and Methods in Physics Research Section B: Beam Interactions with Materials and Atoms, **166-167**, 572-576 (2000). https://doi.org/10.1016/S0168-583X(99)01151-9
[30] B.E. Umirzakov, D.A. Tashmukhamedova, M.K. Ruzibaeva, F.G. Djurabekova, and S.B. Danaev, "Investigation of change of the composition and structure of the CaF_2/Si films surface at the low-energy bombardment," Nuclear Instruments and Methods in Physics Research Section B: Beam Interactions with Materials and Atoms, **326**, 322-325 (2014). https://doi.org/10.1016/j.nimb.2013.10.094
[31] D.A. Tashmukhamedova, and M.B. Yusupjanova, "Formation of Nanoscale Structures on the Surface of MgO Films Upon Bombardment with Low-Energy Ions," Journal of Surface Investigation: X-ray, Synchrotron and Neutron Techniques, **15**(5), 1054-1057 (2021). https://doi.org/10.1134/S1027451021050402

ВПЛИВ ІМПЛАНТАЦІЇ АКТИВНИХ ІОНІВ МЕТАЛІВ НА СКЛАД, ЕМІСІЮ ТА ОПТИЧНІ ВЛАСТИВОСТІ ПЛІВОК MgO

М.Б. Юсупжонова, Д.А. Ташмухамедова, Б.Є. Умірзаков, С.С. Пак, З.Р. Сайдахмедова, Ш.К. Салієва
Ташкентський державний технічний університет імені Іслама Карімова, Ташкент, 100095 Республіка Узбекистан

За допомогою комбінації методів вторинної та фотоелектронної спектроскопії досліджено склад, електронну структуру, емісійні та оптичні властивості плівок MgO/Mg, імплантованих іонами Ba+ та Na+ до та після відпалу. Показано, що після іонної імплантації в поверхневих шарах утворюються аморфні плівки, що складаються із сполук Mg – Ba – O, Mg – O, Ba – O, а також незв'язаних атомів Ba і Mg. При цьому еφ поверхні зменшується. Визначено, що ефективність випромінювання іонно-легованих шарів вища, ніж у шарів MgO. Постімплантаційний відпал при T = 900 K призводить до утворення однорідної плівки $Mg_{0,4}Ba_{0,6}O$ товщиною 30 – 35 Å у разі імплантації іонів Ba+. Виявлено, що глибина виходу фотоелектронів трикомпонентної плівки в 1,5 рази більша, ніж у оксиду Mg. Встановлено основні механізми зміни електронної структури, емісійних та оптичних властивостей MgO під час іонної імплантації та подальшого відпалу.

Ключові слова: *термічне окислення; іонна імплантація; фотоелектронна спектроскопія; квантовий вихід; ефективність еміссії; глибина виходу*